

Uncertainty Analysis for the Measurements of Aerodynamic Loss of Cooled Turbine Blades

S. M. Aminossadati¹, D. J. Mee²

Mechanical Engineering Department
The University of Shahrekord, GPO Box 115, Shahrekord
IRAN
E-mail: aminosadat@yahoo.com

Abstract

The uncertainty analysis is carried out for the aerodynamic loss coefficient of cooled turbine blades based on the accuracy of measured parameters. First, the definition for the aerodynamic loss coefficient is derived. Then, the confidence interval of each measured parameter is determined based on the accuracy of corresponding utilized instrumentation. Finally, by applying the sensitivity of the loss coefficient to each measured parameter, the accuracy of the aerodynamic loss coefficient is calculated. The results show that the loss coefficient is very sensitive to the total pressure measured at a plane downstream of the cooled turbine blades. The uncertainty in the aerodynamic loss coefficient is typically 10%.

Nomenclature

C_m	Ratio of coolant to mainstream mass flow
C_p	Specific heat at constant pressure
E_k	Kinetic energy
K_f	Correction factor (Equation 11)
\dot{m}	Mass flow rate
N	No. of calibration points (Equation 12)
P	Pressure
T	Temperature
v	Velocity
α	Yaw angle
β	Pitch angle
γ	Specific heat ratio
σ	Standard deviation (Equation 11)
ξ	Aerodynamic loss coefficient

Subscripts

1	Upstream conditions
2	Downstream conditions

20	Free-Stream conditions
2'	Traversing plane conditions
3	Mixed-out conditions
A	Probe central hole label (Figure 2)
B,C,D	Probe side holes labels (Figure 2)
atm	Atmospheric condition
c	Coolant flow
dyn	Dynamic
g	Mainstream gas
is	Isentropic
O ₁	Upstream of the orifice plate
O ₂	Downstream of the orifice plate
t	Total (stagnation)

1. INTRODUCTION

Generally, in all experiments, uncertainty analysis is accepted as an important part in examining the test results. Uncertainties occur in the results of any experimental investigation and, hence, it is necessary to identify and estimate them so that a proper assessment of the experimental results can be carried out. One of the benefits of the uncertainty analysis is that the instrumentation and test procedure can then be optimized so as to improve the experimental results. The aerodynamic loss experiments for a cascade of turbine blades or a stationary turbine blade row are derived from a number of separate measurements such as total pressure, velocity and flow angle measurements. Each measurement affects the results to a different degree. The sensitivity of the results to the accuracy of each measurement can then be examined and the most critical measurement can be identified. In this study, the method applied by Miller (1983) and Baines et al. (1991) is used to determine the confidence interval (accuracy) for the aerodynamic loss coefficient of the cooled turbine blades.

¹ Assistant Professor

² Senior Lecturer, Mech. Eng. Dept., The University of Queensland, Australia

2. AERODYNAMIC LOSS COEFFICIENT

The aerodynamic performance of cooled gas turbine blades is generally presented in the form of the kinetic energy loss coefficient.

The kinetic energy loss coefficient is obtained from the kinetic energy efficiency which is the ratio of the kinetic energy of the gas stream at the static pressure at a plane downstream of the cascade, at which the flow is fully mixed out, to that which would be obtained at the mixed-out static pressure if the expansion from the inlet conditions had been isentropic.

$$\xi = 1 - \frac{\text{kinetic energy at the exit}}{\text{ideal kinetic energy}} = 1 - \frac{E_k}{E_{k,is}} \quad (1)$$

The flow upstream and downstream of a cascade of cooled turbine blades is illustrated in Figure 1. It also shows a location downstream of the cascade at which the flow is assumed to be fully mixed-out (mixed-out plane).

In the definition of aerodynamic loss coefficient, for cooled turbine blades, E_k is the actual kinetic energy at the mixed-out static pressure and is given by:

$$E_k = \frac{1}{2} \dot{m}_3 v_3^2 \quad (2)$$

$E_{k,is}$ is the kinetic energy at the mixed-out static pressure if the expansion of the flow was isentropic. For cooled turbine blades, $E_{k,is}$ is given by:

$$E_{k,is} = \frac{1}{2} \dot{m}_g v_{g,is}^2 + \frac{1}{2} \dot{m}_c v_{c,is}^2 \quad (3)$$

Substituting E_k and $E_{k,is}$ in Equation 1 using Equations 2 and 3 results in the final expression for the aerodynamic loss coefficient presented in Equation 4 (see Aminossadati, 1999).

$$\xi = 1 - \frac{\left(1 + \frac{\dot{m}_c C_{pc} T_{tc}}{\dot{m}_g C_{pg} T_{tg}}\right) \left[1 - \left(\frac{P_3}{P_{t3}}\right)^{\frac{\gamma_3-1}{\gamma_3}}\right]}{\left[1 - \left(\frac{P_3}{P_{t1}}\right)^{\frac{\gamma_g-1}{\gamma_g}}\right] + \frac{\dot{m}_c C_{pc} T_{tc}}{\dot{m}_g C_{pg} T_{tg}} \left[1 - \left(\frac{P_3}{P_{tc}}\right)^{\frac{\gamma_c-1}{\gamma_c}}\right]}. \quad (4)$$

The kinetic energy loss coefficient includes the energy of both coolant and mainstream flows and can give a true indication of the aerodynamic loss in cooled gas turbine blades. However, different assumptions can be made to simplify the loss coefficient given by Equation 4. In cases where the coolant and mainstream flows have the same properties (i.e. $C_{pc} = C_{pg}$, $\gamma_c = \gamma_g = \gamma$ & $T_{tc} = T_{tg}$), then,

$$\xi = 1 - \frac{\left(1 + \frac{\dot{m}_c}{\dot{m}_g}\right) \left[1 - \left(\frac{P_3}{P_{t3}}\right)^{\frac{\gamma-1}{\gamma}}\right]}{\left[1 - \left(\frac{P_3}{P_{t1}}\right)^{\frac{\gamma-1}{\gamma}}\right] + \frac{\dot{m}_c}{\dot{m}_g} \left[1 - \left(\frac{P_3}{P_{tc}}\right)^{\frac{\gamma-1}{\gamma}}\right]}. \quad (5)$$

3. LOSS COEFFICIENT UNCERTAINTY

In order to calculate the uncertainty in the loss coefficient, it is necessary to determine the uncertainty in all the measured parameters and the sensitivity of the loss coefficient to each measured parameter.

Equation 5 shows that the aerodynamic loss coefficient is mainly a function of static and total pressures of mainstream flow at the mixed-out plane, total pressure of the flow upstream of the cooled blades, coolant total pressure, and temperatures and mass flow rates of coolant and mainstream flows. The coolant total pressure is calculated at the ejection location according to Kost and Holmes (1985) using continuity, the coolant mass flow and the static pressure into which the coolant is ejected.

Equation 6 shows that the uncertainty in the aerodynamic loss coefficient is a function of the uncertainty in each measured parameter and the sensitivity of the loss coefficient respect to the measured parameters.

$$\begin{aligned} (\delta\xi)^2 = & \left(\frac{\partial\xi}{\partial\alpha_2'}\delta\alpha_2'\right)^2 + \left(\frac{\partial\xi}{\partial\beta_2'}\delta\beta_2'\right)^2 + \left(\frac{\partial\xi}{\partial P_{t2}'}\delta P_{t2}'\right)^2 \\ & + \left(\frac{\partial\xi}{\partial v_2'}\delta v_2'\right)^2 + \left(\frac{\partial\xi}{\partial P_{t1}}\delta P_{t1}\right)^2 + \left(\frac{\partial\xi}{\partial T}\delta T\right)^2 + \left(\frac{\partial\xi}{\partial P_{O1}}\delta P_{O1}\right)^2 \\ & + \left(\frac{\partial\xi}{\partial P_{O2}}\delta P_{O2}\right)^2 + \left(\frac{\partial\xi}{\partial P_{atm}}\delta P_{atm}\right)^2 + \left(\frac{\partial\xi}{\partial P_{dyn,1}}\delta P_{dyn,1}\right)^2 \end{aligned} \quad (6)$$

4. MEASURED PARAMETERS UNCERTAINTY

Conservation equations of mass, momentum and energy are applied to a control volume considered between the traversing plane half a chord downstream of the cooled blades and the mixed-out plane (see Figure 1). Total pressure ($P_{t2'}$), velocity ($v_{2'}$), pitch angle ($\beta_{2'}$) and yaw angle ($\alpha_{2'}$) of the flow at the traversing plane are measured by a four-hole pressure probe and used as the inputs to the conservation equations. Solving these equations yields static pressure (P_3) and total pressure (P_{t3}) of the flow at the mixed-out plane (Aminossadati, 1999).

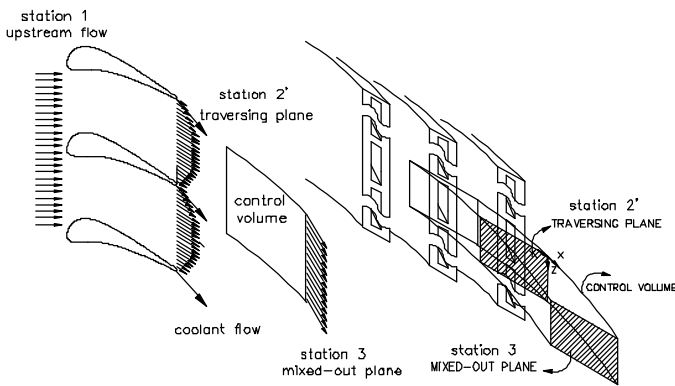


Figure 1 : Flow around a cascade of cooled turbine blades

Thus, the uncertainties in static and total pressures of the flow at the mixed-out plane can be determined by measuring the uncertainties of total pressure, velocity, pitch angle, and yaw angle of the flow at the traversing plane using the four-hole pressure probe.

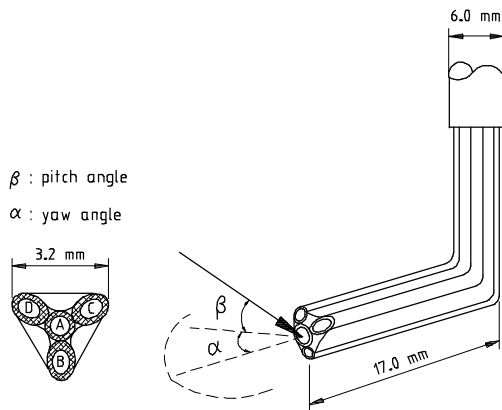


Figure 2 : Probe, showing the hole labeling convention

The probe is a four-hole truncated pyramid probe (Figure 2). The probe has a 6 mm diameter vertical stem. Four stainless steel hypodermic tubes of 1.2 mm outer diameter protrude from the base of this stem, are bent through 90° and protrude 17 mm horizontally. One of the tubes is in the center and the other three tubes are equally spaced around the central tube. The geometry of the tip of the probe is designed to minimize the sensitivity of the probe to Reynolds number. As argued by Shepherd (1981), this can be achieved by designing a sharp-edged probe tip with well-defined separation lines. At low incidence angles, the central hole on the tip of the probe will give a good estimate of the total pressure. The side faces are inclined at 45° to the probe normal, which is similar to the probe used by Shepherd (1981).

The calibration of the probe was performed in the low speed wind tunnel of the Mechanical Engineering Department at the University of Queensland. To support the probe and to set its orientation to the flow during calibration, it was positioned in a manually operated traverse mounted on the top of the test section. There are four differential pressure transducers (SENSYM SCXL004DN) mounted on the top of the probe, which rotate with it. These transducers have a full range of 2.8 kPa. The transducers, with one port open to the atmosphere, were used to measure the probe pressures.

Accuracy of the four-hole probe measurements is studied in terms of errors in the estimated mean values, which include:

1) The errors in the four-hole probe pressure measurements. These errors can be determined based on the uncertainties of the pressure transducers. To estimate the accuracy of the measurements (confidence intervals) of yaw angle (α), pitch angle (β), total pressure (P_t) and velocity (v), the contributions of four pressure transducers to the accuracy of each parameter may be combined by the root-sum-square method (Miller, 1983).

$$Acc.(\alpha) = \pm \sqrt{\left(\frac{\partial \alpha}{\partial P_A} \delta P_A\right)^2 + \left(\frac{\partial \alpha}{\partial P_B} \delta P_B\right)^2 + \left(\frac{\partial \alpha}{\partial P_C} \delta P_C\right)^2 + \left(\frac{\partial \alpha}{\partial P_D} \delta P_D\right)^2} \tag{7}$$

$$Acc.(\beta) = \pm \sqrt{\left(\frac{\partial \beta}{\partial P_A} \delta P_A\right)^2 + \left(\frac{\partial \beta}{\partial P_B} \delta P_B\right)^2 + \left(\frac{\partial \beta}{\partial P_C} \delta P_C\right)^2 + \left(\frac{\partial \beta}{\partial P_D} \delta P_D\right)^2} \tag{8}$$

$$\text{Acc.}(P_t) = \pm \sqrt{\left(\frac{\partial P_t}{\partial P_A} \delta P_A\right)^2 + \left(\frac{\partial P_t}{\partial P_B} \delta P_B\right)^2 + \left(\frac{\partial P_t}{\partial P_C} \delta P_C\right)^2 + \left(\frac{\partial P_t}{\partial P_D} \delta P_D\right)^2} \quad (9)$$

$$\text{Acc.}(v) = \pm \sqrt{\left(\frac{\partial v}{\partial P_A} \delta P_A\right)^2 + \left(\frac{\partial v}{\partial P_B} \delta P_B\right)^2 + \left(\frac{\partial v}{\partial P_C} \delta P_C\right)^2 + \left(\frac{\partial v}{\partial P_D} \delta P_D\right)^2} \quad (10)$$

where, $\frac{\partial \alpha}{\partial P_i}$, $\frac{\partial \beta}{\partial P_i}$, $\frac{\partial P_t}{\partial P_i}$ and $\frac{\partial v}{\partial P_i}$ ($i = A, B, C, D$) are

the sensitivities of the yaw angle, pitch angle, total pressure and velocity measurements to the probe pressures respectively and δP_A , δP_B , δP_C and δP_D are the precision of the transducers, sensing the probe pressures. The sensitivities of yaw angle, pitch angle, total pressure and velocity to the probe pressures were calculated from the calibration application matrix. This was done by perturbing each of the probe hole pressures one at a time and determining the change in the output results of the calibration application matrix (yaw angle, pitch angle, total pressure and velocity).

The precision of each of the four transducers, sensing the pressures of the probe holes (δP_i , $i = A, B, C, D$) can be determined at the 95 percent confidence by using the following expression (Miller, 1983)

$$\delta P_i = K_f \sigma \quad (11)$$

where, K_f is a correction factor and σ is the standard deviation of the calibration data. K_f can be derived from normal distribution for the 95 percent confidence level and it depends on the number of data points. In the present, calculation, a value of 1.96 is used for K_f (Miller, 1983). The standard deviation, σ , is given by

$$\sigma = \left[\frac{\sum (\Delta P_i)^2}{N-1} \right]^{\frac{1}{2}} \quad (12)$$

where, N is the number of calibration points and ΔP_i is the difference between the pressures from the calibration tests and those from the calibration curve. Figure 3 shows the distribution of ΔP_i versus the corresponding calibration pressures for the transducer sensing the pressures of the central hole of the probe. Finally, the accuracy (confidence interval) for total pressure, velocity and yaw and pitch angles, using the 95 percent

confidence, can be calculated by using Equations 7 to 10. The results are presented in the first row of Table 1.

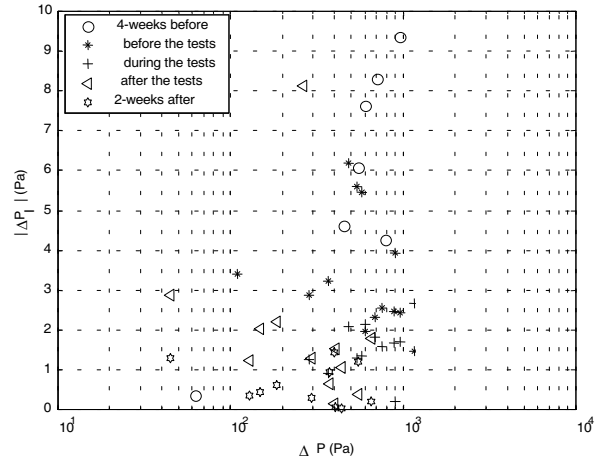


Figure 3: Residual of pressures (ΔP_i) versus the corresponding calibration pressures

2) The errors due to the application of the probe calibration matrix can be estimated by introducing the calibration data as experimental data into the probe application matrix. Then, the differences between the calculated and known values show errors due to the lack of fit of the calibration function. The 95% accuracy (confidence interval) due to the lack of fit in the calibration function are presented in the second row of Table 1.

3) The errors due to the Reynolds number effects may be important especially, when the probe is used in speeds greatly different from the calibration flow speed. To minimize these errors, it is recommended to calibrate the probe over a range of speeds spanning the flow speeds expected in the experiments. As discussed earlier, the Reynolds number effects depend on the geometry of the tip of the probe. In the present experiments, the sharp-edged probe tip with well-defined separation lines ensures minimal sensitivity to Reynolds number. However, to minimize any error due to the Reynolds number effects, the probe was calibrated for a typical flow speed, which is expected in the experiments.

4) The errors due to the high turbulence levels in the free-stream were not included in the present experiments. Even though high turbulence intensity is expected behind the trailing edge of the blade, traversing the probe half a chord downstream of the trailing edge minimizes the influence of turbulence.

5) The 95% accuracy (confidence interval) of pitch and yaw angles due to the alignment of the probe are presented in the third row of Table 1.

Table 1 : Four-hole probe measurements and their 95% confidence intervals

	α (degree)	β (degree)	$\frac{\varepsilon_{P_t}}{0.5\rho v^2}$ (%)	$\frac{\varepsilon_v}{v}$ (%)
Pressure measurements	± 0.2	± 0.2	± 0.8	± 0.7
Calibration fit	± 0.8	± 0.6	± 0.9	± 1.2
Alignment of the probe	± 1.0	± 0.2	0	0
Total	± 1.3	± 0.7	± 1.1	± 1.4

The results shown in Table 1 indicate that the uncertainty in yaw angle is dominated by the uncertainty in alignment of the probe. An improved accuracy in measurement of yaw angle could be obtained by improving the technique used for aligning the probe. The uncertainty in the probe parameters due to the uncertainty in the application of the probe calibration is, in general, higher than that due to uncertainty in the pressure measurements. The total uncertainty in yaw angle, pitch angle, total pressure coefficient, and velocity ratios are $\pm 1.3^\circ$, $\pm 0.7^\circ$, $\pm 1.1\%$ and $\pm 1.4\%$. These values can be used in the uncertainty analysis for experiments in which the four-hole probe is utilized.

The uncertainty in the total pressure upstream of the cooled blades was obtained from the accuracy of a differential pressure transducer (SENSYM SCXL004DN) used to sense this pressure. The uncertainty in coolant mass flow rate was obtained in terms of static pressures upstream and downstream of the orifice plate located in the coolant flow circuit from the accuracy of two pressure transducers (SENSYM SCX30DNC). The uncertainty in the mainstream flow rate was obtained in terms of the dynamic pressure upstream of the cooled blades from the accuracy of Betz manometer used to sense this pressure. The uncertainties in temperatures and atmospheric pressure were obtained from the accuracy of the instruments used to measure these quantities. 95% confidence intervals for these parameters are presented in Table 2.

Table 2: Measured parameters and their 95% confidence intervals

Measured parameters		Confidence intervals
Yaw Angle at the traversing plane	$\alpha_{2'}$	$\delta\alpha_{2'} = \pm 1.3^\circ$
Pitch Angle at the traversing plane	$\beta_{2'}$	$\delta\beta_{2'} = \pm 0.7^\circ$
Total Pressure at the traversing plane	$P_{t2'}$	$\delta P_{t2'} = \pm 6.7 \text{ Pa}$
Flow Velocity at the traversing plane	$v_{2'}$	$\delta v_{2'} = \pm 0.4 \text{ m/s}$
Total Pressure Upstream cascade	P_{t1}	$\delta P_{t1} = \pm 5.5 \text{ Pa}$
Ambient Temperature	T	$\delta T = \pm 0.5^\circ$
Static Pressure Upstream orifice plate	P_{O1}	$\delta P_{O1} = \pm 0.2 \text{ kPa}$
Static Pressure Downstream orifice plate	P_{O2}	$\delta P_{O2} = \pm 0.2 \text{ kPa}$
Atmospheric Pressure	P_{atm}	$\delta P_{\text{atm}} = \pm 10 \text{ Pa}$
Dynamic Pressure Upstream cascade	$P_{\text{dyn},1}$	$\delta P_{\text{dyn},1} = \pm 0.5 \text{ Pa}$

5. LOSS COEFFICIENT SENSITIVITY

The sensitivity of the loss coefficient to each measured parameter is a partial derivative. There is no analytical method of calculating the values of the partial derivatives in Equation 6. However, each partial derivative can be approximated numerically. This can be done by individually perturbing each measured parameter and recording the differences in the loss coefficient relative to the baseline. Table 3 shows the perturbations for each parameter.

Table 3: The perturbations for each measured parameter

Measured parameter	Perturbation
$\alpha_{2'}$	$\partial\alpha_{2'} = 2^\circ$
$\beta_{2'}$	$\partial\beta_{2'} = 2^\circ$
$P_{t2'}$	$\partial P_{t2'} = 20 \text{ Pa}$
$v_{2'}$	$\partial v_{2'} = 1 \text{ m/s}$
P_{t1}	$\partial P_{t1} = 20 \text{ Pa}$
T	$\partial T = 2^\circ \text{ C}$
P_{O1}	$\partial P_{O1} = 2 \text{ kPa}$
P_{O2}	$\partial P_{O2} = 2 \text{ kPa}$
P_{atm}	$\partial P_{\text{atm}} = 100 \text{ Pa}$
$P_{\text{dyn},1}$	$\partial P_{\text{dyn},1} = 5 \text{ Pa}$

By introducing the uncertainties and the calculated partial derivatives (sensitivities) into Equation 6, the uncertainty in the loss coefficient can be determined. The results show that the loss coefficient is very sensitive to the total pressure upstream of the cascade and total pressure and velocity of the flow at the traversing plane. The uncertainties in other parameters have negligible effects on the loss coefficient. As an example, Table 4 shows the contributions to the uncertainty in the loss coefficient due to the uncertainty in each measured parameter at one experimental condition.

Table 4: Contributions to the uncertainty in loss coefficient

Measured parameter	$\alpha_{2'}$	$\beta_{2'}$	$P_{t2'}$	$v_{2'}$	P_{t1}
$\delta\xi_i$	6×10^{-4}	3×10^{-5}	5×10^{-3}	1×10^{-3}	2×10^{-3}
Measured parameter	P_{O2}	P_{O1}	T	P_{atm}	$P_{dyn,1}$
$\delta\xi_i$	2×10^{-4}	2×10^{-4}	1×10^{-4}	1×10^{-5}	6×10^{-5}

The uncertainty analysis was repeated for all data set and the results are presented in Figure 4.

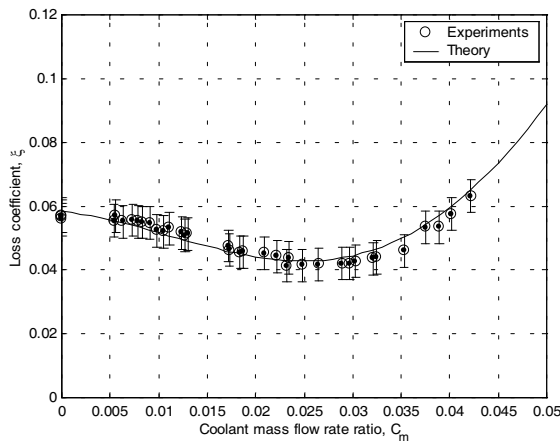


Figure 4: Error bars presented on the values of aerodynamic loss coefficient

The results for five tests at different coolant mass flow rate ratios are also presented in Table 5. The uncertainty in the loss coefficient is typically 10% of the loss for zero blowing rate. The relative uncertainty rises to about 12.5% at the lowest level of loss measured. The major contributor to the uncertainty is the error in the total pressure measured at the traversing plane ($P_{t2'}$). In the present tests, it was possible to get this as low as 6.7 Pa to achieve the final uncertainty in loss coefficient presented in Table 5.

Table 5: The loss coefficient uncertainty

C_m	ξ	$\delta\xi$	% Uncertainty
0.0000	0.0568	± 0.0054	9.5
0.0063	0.0552	± 0.0050	9.1
0.0209	0.0452	± 0.0051	11.3
0.0260	0.0417	± 0.0052	10.3
0.0375	0.0533	± 0.0055	10.3

6. CONCLUSION

In the present study, the uncertainty in the aerodynamic loss coefficient was studied in terms of the uncertainties in measured parameters and the sensitivity of loss coefficient to each parameter. The results indicate the accuracy of the loss coefficient for each measured point. This can be used for a better study of the loss coefficient variation. For the present loss coefficient results, the uncertainty in the loss coefficient is typically 10%.

7. ACKNOWLEDGMENT

The authors would like to thank the mechanical engineering department of the university of Queensland for providing the wind tunnel and the calibration rig.

8. REFERENCES

- 1) Aminossadati S.M., (1999), "Simulation of aerodynamic loss for turbine blades with trailing edge coolant ejection", PhD Thesis, The University of Queensland, Australia.
- 2) Baines N.C., Mee D.J., Oldfield M.L.G. (1991), "Uncertainty analysis in turbomachine and cascade testing", International Journal of Engineering Fluid Mechanics, Vol. 4, No. 4, PP 375-401.
- 3) Kost F.H. and Holmes A.T. (1985), "Aerodynamic effect of coolant ejection in the rear part of transonic rotor blades", AGARD-CP-390, Paper No. 41.
- 4) Miller R.W. (1983), "Flow measurement engineering handbook", McGraw Hill, New York, USA.
- 5) Shepherd I.C. (1981), "A four-hole pressure probe for fluid flow measurements in three dimensions", ASME Journal of Fluids Engineering, Vol. 103, No. 4, PP. 590-594.